BMC Medical Imaging

RESEARCH

Open Access

Assessment of cardiac iron deposition and genotypic classification in pediatric beta-thalassemia major: the role of cardiac MRI

Siqi Zhang[1,2†], Wen Zhao[2†], Longwei Sun[2], Guohua Liang[2], Xiaodong Wang[3] and Hongwu Zeng[2*]

Abstract

Background Beta thalassemia major (β-TM) is a severe genetic anemia with considerable phenotypic heterogeneity. This study investigated whether genotype correlates with distinct myocardial iron overload patterns, assessed by cardiovascular magnetic resonance (CMR) T2* values.

Methods CMR data for cardiac iron deposition evaluation, which recruited pediatric participants between January 2021 and December 2024, were analyzed with CVI42. The patients were classified into three genetic subgroups of β^0/β^0, β^0/β^+, and β^+/β^+ based on their genetic outcomes. The CMR results classified patients into normal myocardial T2* value and myocardial iron overload groups. Qualitative and quantitative factors were subsequently compared by groups using comparative statistics.

Results The study included 145 pediatric β-TM patients, with 24 (17%) exhibiting cardiac iron deposition based on CMR T2* values. There were significant differences in iron chelation treatment strategies across genotypes, with the β^0/β^0 genotype accounting for 54% (13/24) of patients in the cardiac iron deposition group. Regardless of genotype, the mid-inferolateral segment consistently showed the lowest CMR T2* values and the highest prevalence of iron deposition.

Conclusion The risk of cardiac iron deposition increases as age progresses, and the mid-inferolateral segment is more susceptible to iron accumulation. The β^0/β^0 genotype is more likely to suffer from cardiac iron overload, emphasizing the need for closer clinical monitoring and regular cardiac MRI evaluations.

Keywords B-thalassemia major, Cardiac MRI, Iron deposition, Genotype, Paediatric

†Siqi Zhang and Wen Zhao contributed equally to this work.

*Correspondence:
Hongwu Zeng
homerzeng@126.com
[1]Department of Radiology and Nuclear Medicine, Xuanwu Hospital Capital Medical University, Beijing 100053, China
[2]Department of Radiology, Shenzhen Children's Hospital, Shantou University Medical College, 7019 Yitian Road, Futian District, Shenzhen 518038, China
[3]Department of Hematology and Oncology, Shenzhen Children's Hospital, 7019 Yitian Road, Futian District, Shenzhen 518038, China

Introduction

Thalassemia is an inherited hemolytic anemia resulting from mutations in globin synthesis. Among the various forms, beta-thalassemia major (β-TM) is the most notable and severe genetic phenotype, affecting approximately 1.5% of the global population [1]. β-TM is characterized by a deficiency in the β chains of hemoglobin, resulting in anemia that requires regular transfusions and subsequent iron overload [2]. Dysregulation of iron homeostasis is a central feature of thalassemia pathophysiology. Cardiac complications (such as heart failure) due to iron overload are the primary cause of morbidity and mortality in β-TM patients [3, 4]. Neither organ biopsy (an invasive procedure) nor serum ferritin (which fluctuates with many variables), could estimate myocardial iron content directly. Conventional assessments such as ultrasound could only identify patients with advanced disease [5].

Cardiac magnetic resonance imaging (CMR) T2* is significant in the non-invasive and highly reproducible quantification for evaluating cardiac iron loading. This assessment is the strongest predictor of cardiac complications [6] and has significantly improved survival rates in β-TM patients [7]. As a result, CMR is now routinely recommended for assessing iron overload in pediatric β-TM patients, according to major clinical guidelines [8]. CVI42® (Circle Cardiovascular Imaging, www.circlecvi.com) is FDA and European Community-approved and effectively measures CMR T2* [9]. It automatically identifies ROIs to generate accurate T2* decay curves, although its clinical use is limited by cost [10]. Nonetheless, it is valuable for accurately reporting iron content.

Due to extensive molecular heterogeneity, β-TM patients exhibit a wide range of clinical presentations [11]. While the correlation between phenotype and genotype is intricate [12], the genetic component has been established as a prognostic risk factor for β-TM patients [13], potentially contributing to varying levels of cardiac impairment [14]. Previous research has confirmed that diverse patterns of cardiac iron overload are associated with different prognoses [15]. However, the detailed relationship between cardiac iron overload patterns and genetic subtypes remains unclear. Therefore, we aimed to evaluate the distribution of cardiac iron deposition in different genotypic groups of pediatric β-TM, assessed through CMR T2*.

Methods

Participants

We retrospectively reviewed patients undergoing CMR evaluation for cardiac iron deposition from January 2021 to December 2024. Inclusion criteria: (1) availability of complete baseline clinical data; (2) no prior hemopoietic stem-cell transplantation treatment; (3) diagnosis confirmed by genetic analysis. Exclusion criteria: (1) anemia resulting from causes other than β-TM; (2) cases with incomplete or insufficient clinical data. 145 children were ultimately included in this retrospective study, approved by the Ethics Committee of Shenzhen Children's Hospital (No. 202004002). Figure 1 illustrates the workflow for patient selection.

Clinical data included sex, age, and chelation therapy details, with confirmation of monotherapy or combination therapy using deferoxamine (DFO), deferasirox (DFX), or deferiprone (DFP). Peripheral blood samples were collected, and laboratory tests measured serum ferritin (ng/ml), hemoglobin (g/L), and hematocrit (%). β-thalassemia mutations were identified using a reverse hybridization assay (β-globin strip assay, Shenzhen Children's Hospital Lab). The β^+ mutations included IVS-II-654, -28, βE, -29, -30, -32, CAP, and IVS-I-5, while the β^0 mutations consisted of CD41-42, CD17, CD71-72, Int, CD31, CD14-15, IVS-I-1, CD43, and CD27-28. Based on these genetic results, patients were classified into three subgroups β^0/β^0, β^0/β^+, and β^+/β^+.

MRI acquisition

CMR exams were performed using a 1.5T scanner (GE, Signa, USA). An eight-element cardiac phased-array receiver surface coil with breath holding in end-expiration and ECG-gating was used. To measure myocardial T2*, a single short-axis mid-ventricular slice was acquired at nine echo times (TE min full) [16]. A gating delay time of 0ms after the R-wave was chosen to obtain myocardial images consistently in the cardiac cycle irrespective of the heart rate. A full-thickness region of interest was measured in the left ventricular myocardium, encompassing both epicardial and endocardial regions. The detailed sequence parameters can be found in the Supplementary Table 1.

Image postprocessing

CMR T2* is a method for assessing tissue iron content and demonstrates an inverse correlation with iron levels, making it valuable for diagnosing myocardial iron deposition. For image analysis and T2* measurement, CVI42 version 5.17.1 (Circle Cardiovascular Imaging, Canada) was used. This software provided T2* values for six segments of the short-axis mid-ventricular slice of the left ventricle: anterior, anteroseptal, inferoseptal, lateral, inferolateral, and anterolateral. After the post-processing software identifies the ROIs, two radiologists specializing in pediatric cardiac imaging (ZW, with 5 years of experience; SLW, with 25 years of experience) collaboratively review all ROI boundaries to ensure accuracy.

The global heart T2* value was obtained by averaging the values of all six segments. The segment most susceptible to iron overload had the lowest T2* value among the

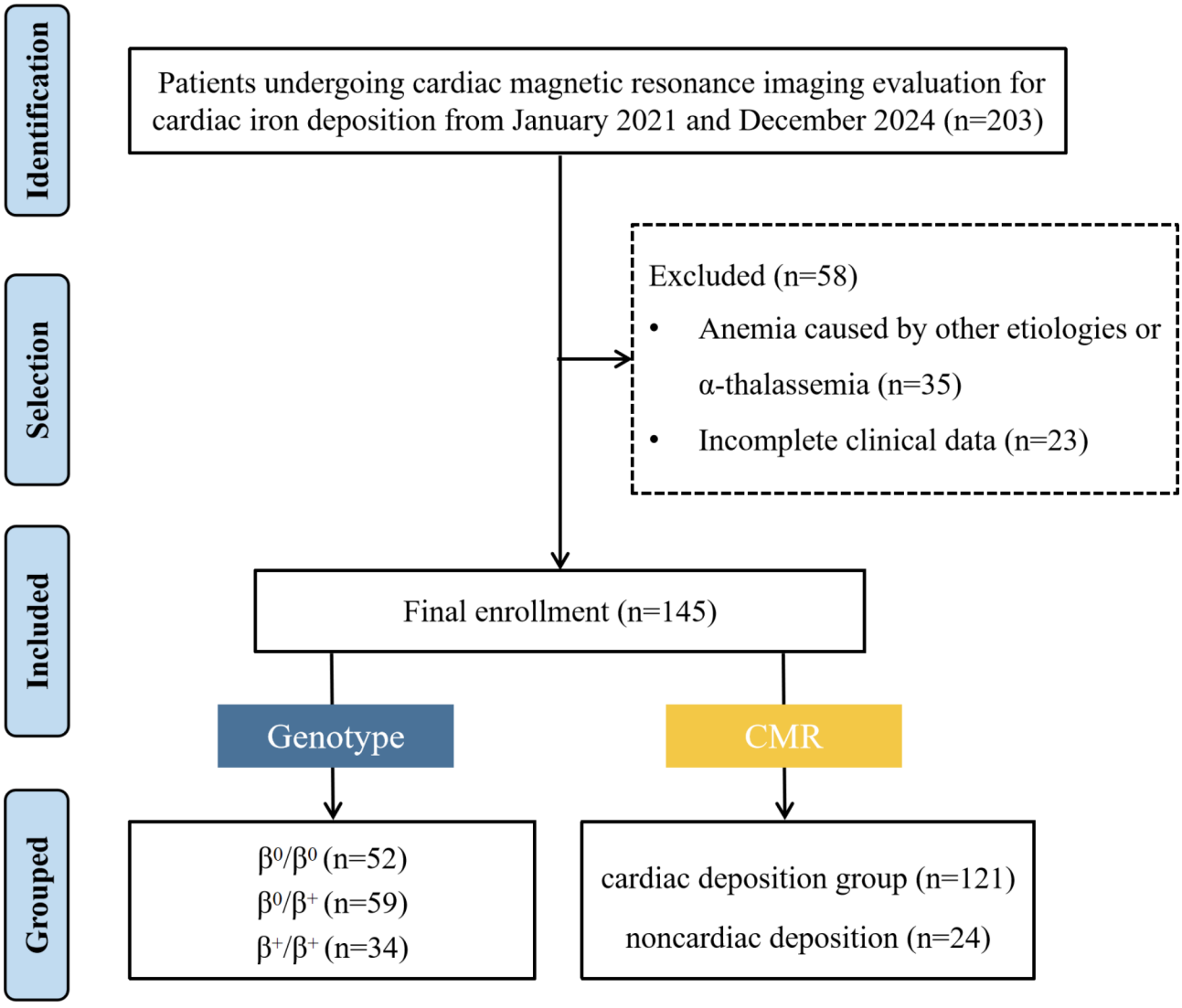

Fig. 1 Flowchart of patient selection

six segments for each patient. Patients were then categorized as having normal heart iron concentration (T2* > 20 ms) or cardiac iron deposition (T2* ≤ 20 ms), based on previously published guidelines [17]. Left ventricular (LV) function parameters for each patient were obtained using cine sequences, including left ventricular ejection fraction (LVEF), cardiac output (CO), end-diastolic volume index (EDVI), end-systolic volume index (ESVI), and stroke volume (SV).

Statistical analysis

SPSS 27.0 (IBM, New York, USA) statistical analysis software was used for data analysis. The normality of continuous parameter distributions was assessed using the Kolmogorov-Smirnov test. Normally distributed data were described as mean (standard deviation), while non-normally distributed data were expressed as median (interquartile range). For continuous variables, comparisons among the three groups were conducted using the One-Way ANOVA test when they had a normal distribution and the Kruskal-Wallis test when they exhibited a non-normal distribution. Independent samples *t* test and Mann-Whitney U test were utilized to analyze differences between the two groups. Categorical variables were presented as frequencies and percentages, and the chi-square test was employed for analysis. Post-hoc analysis using the Bonferroni correction was performed for comparisons with significant intergroup differences. A *p*-value of < 0.05 was statistically significant.

Results

Demographics in beta genotypes

Throughout the observation period, 203 patients who underwent CMR T2* were enrolled. Fifty-eight patients

were excluded due to other etiologies or incomplete data, leaving 145 patients for final inclusion. The demographic and clinical characteristics of the patients across the three genotypic groups are summarized in Table 1. Three groups of patients were identified: β^0/β^0 ($n=52$), β^0/β^+ ($n=59$), β^+/β^+ ($n=34$). Significant differences were observed in hematocrit levels ($p=0.049$), chelation therapy ($p=0.041$), and combined/sequential therapy frequency ($p=0.038$) among the genetic subtypes (Fig. 2a-c). The analysis also revealed that β^0/β^+ patients were more likely to receive DFX monotherapy (63% vs. 38% and 56%, $p<0.05$), whereas β^0/β^0 patients were more commonly treated with dual chelation therapy (37% vs. 20% and 3%, $p<0.05$).

CMR features in beta genotypes

The CMR features in the three genotypic groups are summarized in Table 2. The median global heart T2* value was 34ms (range 4.7–59.5) with an interquartile range of 10ms. Among the 145 included patients, 24 (16.6%) had cardiac iron deposition. Figure 3 displays examples showing varying degrees of myocardial siderosis as assessed by CVI42. In the cardiac iron deposition group, the β^0/β^0 genotype was more prevalent, accounting for 54% (13/24), and was more likely to experience iron overload compared to the other genotypes (25% vs. 10% vs. 15%), although this difference was not statistically significant.

Further analysis revealed that isolated segment myocardial iron deposition was most common, accounting for 17%, 31%, and 35% in the three genetic subtypes, respectively. Among the six mid-cardiac segments, the inferolateral segment showed the lowest CMR T2* values and the highest prevalence of iron deposition, with proportions of 40%, 49%, and 35% in the three genetic subtypes (Fig. 2d-e). No significant differences were found in the iron deposition distribution patterns or cardiac function parameters among the three genetic subtypes (β^0/β^0, β^0/β^+, and β^+/β^+).

Cardiac iron overload

Table 3 summarizes the clinical and radiological factors of the groups with and without cardiac iron deposition. Patients who suffered cardiac iron deposition were older than those in the normal group (mean age of 12.8 years vs. 10.9 years, $p=0.004$) (Fig. 2f). The distribution of chelation therapy differed statistically between the two groups ($p=0.012$) (Fig. 2g). Patients without cardiac iron deposition were more likely to receive monotherapy (76% vs. 50%, $p<0.05$). In contrast, patients with cardiac iron deposition typically underwent combination therapy involving three medications (13% vs. 3%, $p<0.05$). There were no significant differences in sex, laboratory indicators, genotype, or cardiac function between the two groups.

Table 1 Demographics in the three genotypic groups

Parameters/variables	Genotype			*p*-Value
	β^0/β^0 ($n=52$)	β^0/β^+ ($n=59$)	β^+/β^+ ($n=34$)	
Age [a] (years)	11.6 (3.1)	10.8 (2.8)	11.4 (3.1)	0.351
Sex [c] (M/F)	29 / 23	40 / 19	19 / 15	0.349
Serum ferritin [b] (ng/ml)	2720 (3221)	2218 (2286)	2878 (4070)	0.162
Hemoglobin [a] (g/L)	105.2 (18.6)	100.3 (14.5)	97.5 (17.6)	0.094
Hematocrit [a] (%)	30.8 (5.8)[e]	29.7 (4.5)	27.8 (6.7)[e]	0.049[d]
Chelation therapy [c] (%)				0.041[d]
DFO	10 (50)	7 (35)	3 (15)	
DFX	20 (26)[e]	37 (49)[e]	19 (25)	
DFP	1 (13)	2 (25)	5 (62)	
DFO + DFX	13 (50)	9 (35)	4 (15)	
DFO + DFP	2 (67)	1 (33)	0	
DFX + DFP	4 (67)	2 (33)	0	
DFO + DFX + DFP	2 (33)	1 (17)	3 (50)	
Number of chelation therapy types [c] (%)				0.038[d]
One	31 (30)	40 (44)	21 (26)	
Two	19 (54)[e]	12 (34)	1 (12)[e]	
Three	2 (33)	1 (17)	3 (50)	

a. Data are mean, with standard deviation. The One-Way ANOVA test was used to analyze

b. Data are median, with interquartile range. The Kruskal-Wallis test was used to analyze

c. Data are frequency, with percentage. The Chi-square test was used to analyze

d. A p-value of <0.05 was statistically significant

e. Post-hoc analysis (Bonferroni correction) showed a significant difference between the two groups ($p<0.05$)

f. DFO: deferoxamine; DFX: deferasirox; DFP: deferiprone

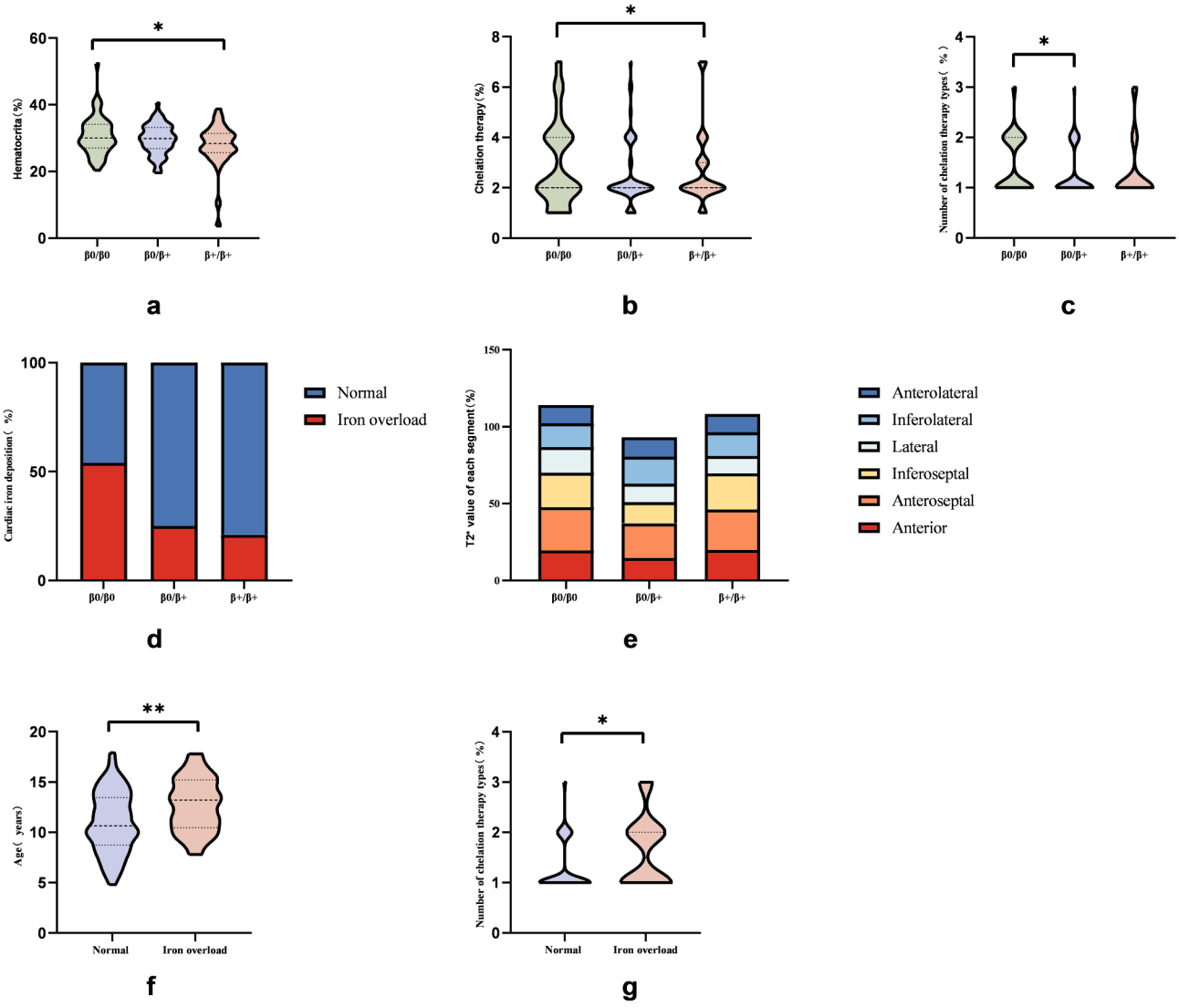

Fig. 2 Visualization of significant intergroup differences in statistical indicators. * and ** indicate statistically significant *p*-values of < 0.05 and < 0.01, respectively

Discussion

Blood transfusions cause iron deposition in the heart, liver, and other organs, leading to cardiac siderosis and cardiomyopathy, which is the major cause of β-TM patient death [3]. Fortunately, this complication is reversible with appropriate iron chelation therapy, highlighting the need for monitoring cardiac iron overload [4]. While serum ferritin levels are unreliable due to various influencing factors, tissue biopsy is accurate but invasive and subject to uneven iron distribution. CMR T2* using the gradient-echo relaxometry method has been validated as a non-invasive, simple, and reliable method to assess myocardial iron overload [5].

Our study included 145 β-TM patients who depended on long-term blood transfusions. In the course of patient analysis, both the global cardiac iron overload and the iron distribution in each cardiac segment (the short-axis mid-ventricular slice) were evaluated using CVI42. The dataset was further grouped as cardiac iron deposition and noncardiac iron deposition based on the CMR T2* value. According to our findings, 16.6% of pediatric patients exhibited abnormal cardiac iron deposition (T2* < 20ms), which is slightly lower than the previously reported data suggesting that 17-40% of children with β-TM experienced cardiac iron overload [18–21]. The differences in measurement tools and ROI ranges may account for the lower proportion of cardiac iron overload in this study. Interestingly, we observed a significantly lower mean age in the noncardiac iron deposition group compared to the cardiac iron deposition group, consistent with previous research [18, 21]. As β-TM patients undergo long-term regular blood transfusions, the risk

Table 2 CMR features in the three genotypic groups

Parameters/variables	Genotype			*p*-Value
	β^0/β^0 ($n=52$)	β^0/β^+ ($n=59$)	β^+/β^+ ($n=34$)	
Global heart T2* value [b] (ms)	34.7 (14.7)	34.1 (8.4)	33.4 (10.8)	0.997
Cardiac iron deposition [c] (%)	13 (54)	6 (25)	5 (21)	0.105
T2* value of each segment (ms)				
Anterior [b]	36.4 (19.6)	36.3 (14.7)	34.4 (19.9)	0.943
Anteroseptal [b]	39.4 (28.1)	38.8 (22.5)	44.9 (26.3)	0.531
Inferoseptal [b]	38.7 (22.4)	38.3 (13.7)	36.3 (23.5)	0.819
Lateral [a]	32.2 (16.7)	30.7 (12.1)	28.7 (11.2)	0.513
Inferolateral [b]	24.9 (15.3)	26.4 (17.4)	23.5 (15.4)	0.529
Anterolateral [a]	30.0 (12.0)	32.3 (12.7)	30.7 (11.9)	0.589
The most susceptible segment to iron deposition [c] (%)				0.642
Anterior	6 (32)	8 (42)	5 (26)	
Anteroseptal	2 (50)	0 (0)	2 (50)	
Inferoseptal	1 (17)	2 (33)	3 (50)	
Lateral	12 (37.5)	12 (37.5)	8 (25)	
Inferolateral	21 (34)	29 (47)	12 (19)	
Anterolateral	10 (46)	8 (36)	4 (18)	
Number of segments with T2* < 20ms [c] (%)				0.570
Zero	30 (41)	31 (42)	13 (17)	
One	9 (23)	18 (46)	12 (31)	
Two	2 (29)	2 (29)	3 (42)	
Three	1 (33)	1 (33)	1 (33)	
Four	1 (33)	2 (67)	0 (0)	
Five	4 (50)	1 (13)	3 (37)	
Six	5 (46)	4 (36)	2 (18)	
Cardiac function				
LVEF [b] (%)	63 (10)	65 (10)	62 (10)	0.109
CO [b] (L/min)	3.2 (1.0)	3.6 (1.4)	3.3 (0.9)	0.267
EDVI [b] (ml/m^2)	43.8 (16.6)	49.1 (19.7)	46.7 (23.5)	0.545
ESVI [b] (ml/m^2)	16.7 (6.5)	17.4 (7.6)	21.9 (11.4)	0.072
SV [a] (ml)	35.8 (12.4)	36.3 (11.6)	33.1 (11.2)	0.426

a. Data are mean, with standard deviation. The One-Way ANOVA test was used to analyze

b. Data are median, with interquartile range. The Kruskal-Wallis test was used to analyze

c. Data are frequency, with percentage. The Chi-square test was used to analyze

d. A p-value of <0.05 was statistically significant

e. Post-hoc analysis (Bonferroni correction) showed a significant difference between the two groups ($p<0.05$)

f. DFO: deferoxamine; DFX: deferasirox; DFP: deferiprone; LVEF: left ventricular ejection fraction; CO: cardiac output; EDVI: end-diastolic volume index; ESVI: end-systolic volume index; SV: stroke volume

of organ iron deposition increases with aging and cumulative transfusion exposure. The outcomes further confirmed the importance of early detection and regular follow-up for cardiac iron deposition in β-TM patients.

Genotypic variations could lead to diverse degrees of cardiac iron accumulation. Our study outcomes revealed that the β^0/β^0 group took up the highest proportion (54%) among pediatric β-TM patients with cardiac iron deposition, consistent with the findings of Zhou et al. [18]. The increased susceptibility to iron toxicity-induced DNA damage of the β^0/β^0 genotype [11] could potentially account for the association with the heightened risk of cardiac iron overload [13]. Irrespective of the global heart T2* value, a noteworthy proportion of patients demonstrate a heterogeneous myocardial iron burden. Within the cohort, 49% of individuals exhibit iron overload in at least one myocardial segment, a prevalence far surpassing those identified as having cardiac iron deposition based solely on the global heart T2* value (17%). This finding was in line with the previous research [15] and underscored the significance of evaluating the distribution of T2* values in each myocardial segment.

In iron overload cardiomyopathy, iron predominantly deposits in the subepicardial fibers [22]. Our results also revealed that the mid-inferolateral segment exhibited the lowest CMR T2* values and the highest prevalence of iron deposition, regardless of genotype in β-TM children. A similar pattern was observed in the heterogeneous

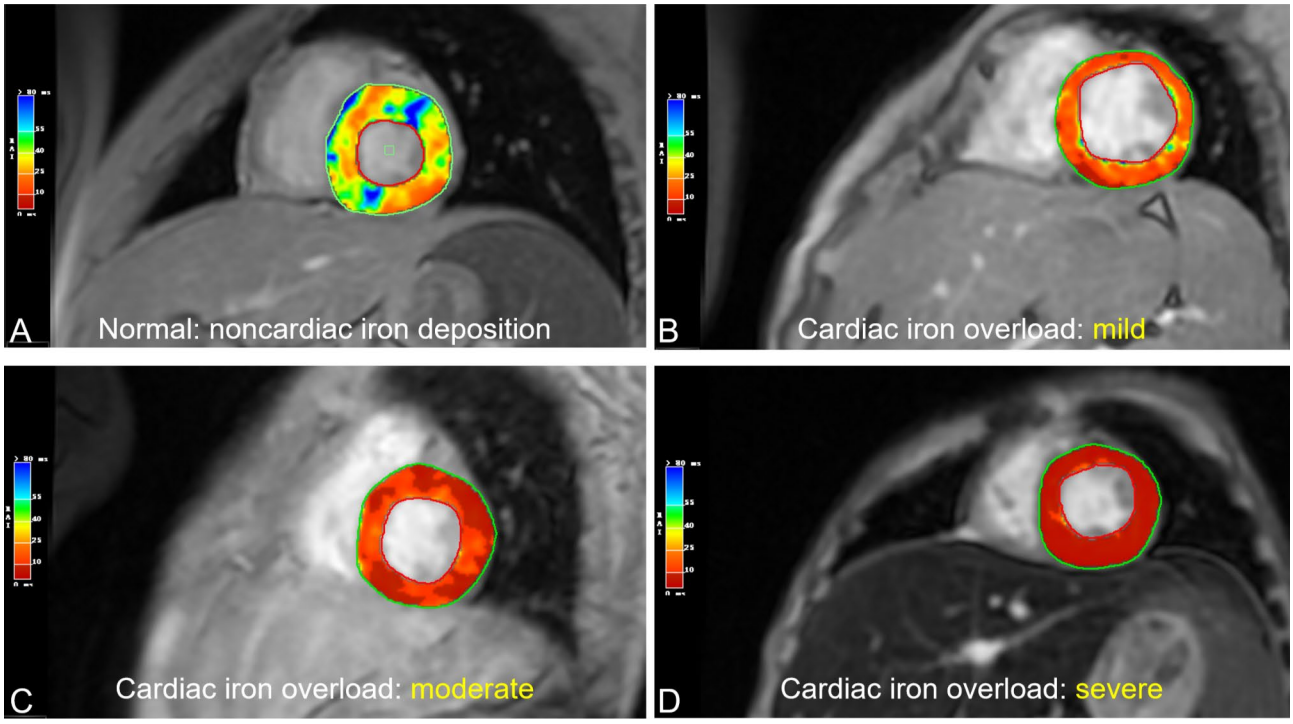

Fig. 3 Patients with different degrees of myocardial siderosis accessed by CVI42. The color overlaid on the images of the T2* mapping sequence. (**A**) The example of a noncardiac iron deposition patient with a global heart T2* value of 37.5 (T2* > 20ms). (**B**) The example of mild cardiac iron deposition patient with a global heart T2* value of 18.3 (14ms < T2* ≤ 20ms). (**C**) The example of moderate cardiac iron deposition patient with a global heart T2* value of 11.4 (10ms < T2* ≤ 14ms). (**D**) The example of severe cardiac iron deposition patient with a global heart T2* value of 6.3 (T2* ≤ 10ms)

myocardial iron overload model proposed by Meloni et al. [15], although their study primarily focused on the heterogeneity aspect and did not include segment-level analysis. Our study provides a more detailed analysis of the segmental distribution of cardiac iron deposition. While statistical significance may be limited due to sample size, it is important to note the higher risk of iron accumulation in the inferolateral segment, which warrants targeted monitoring and treatment.

Prolonged high iron levels can lead to tissue toxicity and endocrine abnormalities, necessitating essential iron chelation for pediatric β-TM patients [8]. The data regarding chelation therapy showed a higher prevalence of monotherapy with DFX in each subtype compared to the other two drugs. This preference was attributed to its superior adherence rates [23, 24], which is particularly important among adolescent patients [25]. Moreover, DFP therapy was more frequent in the β^+/β^+ genotype when compared other two groups, since DFP is well known for being more effective in removing iron from the heart [26]. In transfusion-dependent patients who began regular transfusions during early childhood, combined chelation therapy has significantly outperformed any single drug treatment in reducing organ iron [27]. Consequently, the present study observed a marked increase in the usage of combination therapy among individuals in the β^0/β^0 genotype group and those diagnosed with cardiac iron deposition.

This study has several potential limitations. First, it is limited by its retrospective design, the small number of patients with myocardial iron overload, and the single-center setting. Future studies will aim to expand the cohort or incorporate multicenter data to further validate and strengthen the findings. Second, our analysis focused on six myocardial segments rather than a comprehensive assessment of the entire heart. However, previous research [28] has demonstrated that iron content in the interventricular septum largely reflects the iron content of the whole heart. Third, the considerable heterogeneity in individual iron chelation therapy may introduce bias in result interpretation, despite the absence of a clear consensus on treatment adherence or the optimal measurement methods [25]. Finally, this study did not account for the potential influence of transfusion history on iron deposition, which will be addressed in future research.

Conclusions

In conclusion, our clinical analysis demonstrates a significant correlation between cardiac iron deposition and advancing age. The β^0/β^0 genotype is notably associated with a higher prevalence of myocardial iron overload. Segmental heart T2* analysis revealed distinct patterns of cardiac iron distribution, with the likelihood of iron

Table 3 Comparison of indicators between groups with and without cardiac iron deposition

	Normal myocardial T2* ($n=121$)	Cardiac iron deposition ($n=24$)	*p*-Value
Age [a] (years)	10.9 (3.0)	12.8 (2.7)	0.004[d]
Sex [c] (M/F)	71 / 50	17 / 7	0.265
Serum ferritin [b] (ng/ml)	2558 (22876.5)	3323 (4442)	0.095
Hemoglobin [a] (g/L)	101.9 (17.1)	99.0 (16.5)	0.452
Hematocrit [a] (%)	29.8 (5.7)	28.8 (5.3)	0.435
Chelation therapy [c]			0.097
DFO (%)	16 (80)	4 (20)	
DFX (%)	69 (91)	4 (9)	
DFP (%)	7 (88)	1 (12)	
DFO + DFX (%)	16 (73)	6 (27)	
DFO + DFP (%)	2 (67)	1 (33)	
DFX + DFP (%)	5 (83)	1 (17)	
DFO + DFX + DFP (%)	3 (50)	3 (50)	
Number of chelation therapy types [c] (%)			0.012[d]
One	92 (88)[e]	12 (12)[e]	
Two	26 (74)	9 (26)	
Three	3 (50)[e]	3 (50)[e]	
Genotype [c] (%)			0.105
β^0/β^0	39 (75)	13 (25)	
β^0/β^+	53 (90)	6 (10)	
β^+/β^+	29 (85)	5 (15)	
Cardiac function			
LVEF [b] (%)	63 (10)	65 (10)	0.285
CO [b] (L/min)	3.4 (1.0)	3.4 (1.1)	0.811
EDVI [b] (ml/m^2)	46.2 (19.9)	45.7 (16.6)	0.455
ESVI [b] (ml/m^2)	17.8 (8.2)	17.2 (7.2)	0.962
SV [a] (ml)	35.2 (11.5)	36.1 (13.5)	0.743

a. Data are mean, with standard deviation. The independent samples *t* test was used to analyze

b. Data are median, with interquartile range. The Mann-Whitney U test was used to analyze

c. Data are frequency, with percentage. The Chi-square test was used to analyze

d. A *p*-value of < 0.05 was statistically significant

e. DFO: deferoxamine; DFX: deferasirox; DFP: deferiprone; LVEF: left ventricular ejection fraction; CO: cardiac output; EDVI: end-diastolic volume index; ESVI: end-systolic volume index; SV: stroke volume

deposition in individual segments being much higher than that indicated by the global heart T2* value. Specifically, the mid-inferolateral segment exhibited a marked propensity for iron accumulation. These findings highlight the importance of considering genotype-specific iron deposition patterns in clinical management and chelation strategies for pediatric β-TM patients and recommend incorporating cardiac MRI assessments into the follow-up of β^0/β^0 patients. Future cohort studies with expanded sample sizes will be conducted to further validate our results.

Abbreviations

β-TM Beta thalassemia major
CMR Cardiovascular magnetic resonance
DFO Deferoxamine
DFP Deferipronecf
DFX Deferasirox

Supplementary Information

The online version contains supplementary material available at https://doi.org/10.1186/s12880-025-01567-7.

Supplementary Material 1

Author contributions

Siqi Zhang and Wen Zhao contributed equally to this work. Siqi Zhang and Wen Zhao conceived the paper and prepared the manuscript. Wen Zhao, Longwei Sun, Guohua Liang performed MRI examinations and analyzed data. Xiaodong Wang collected clinical data of patients. Siqi Zhang wrote and edited the manuscript. Hongwu Zeng revised the manuscript. All authors read and approved the final manuscript.

Funding

This work was supported by the Sanming Project of Medicine in Shenzhen (SZSM202011005) from Shenzhen Medical and Health Project and the Guangdong High-level Hospital Construction Fund (ynkt2021-zz47).

Data availability

The data that support the findings of this study are available from the corresponding author upon reasonable request.

Declarations

Ethics approval
Ethical approval: The studies involving human participants were reviewed and approved by the Medical Ethics Committee of the local hospital (No. 202004002).

Informed consent
All the participants and guardians of adolescents signed a written informed consent form after receiving a complete study description.

Consent for publication
Not applicable.

Competing interests
The authors declare no competing interests.

Submission declaration and verification
The work described has not been published previously and is not under consideration for publication elsewhere.

Artificial intelligence
While preparing this work, the authors didn't use any tools for article writing.

Received: 9 November 2024 / Accepted: 22 January 2025
Published online: 30 January 2025

References
1. Kattamis A, Kwiatkowski JL, Aydinok Y. Thalassaemia. Lancet. 2022;399(10343):2310–24. https://doi.org/10.1016/S0140-6736(22)00536-0
2. Motta I, Bou-Fakhredin R, Taher AT, Cappellini MD. Beta thalassemia: new therapeutic options beyond transfusion and iron chelation. Drugs. 2020;80(11):1053–63. https://doi.org/10.1007/s40265-020-01341-9
3. Pepe A, Meloni A, Rossi G, Midiri M, Missere M, Valeri G, Sorrentino F, D'Ascola DG, Spasiano A, Filosa A, et al. Prediction of cardiac complications for Thalassemia major in the widespread cardiac magnetic resonance era: a prospective multicentre study by a multi-parametric approach. Eur Heart J Cardiovasc Imaging. 2018;19(3):299–309. https://doi.org/10.1093/ehjci/jex012
4. Musallam KM, Barella S, Origa R, Ferrero GB, Lisi R, Pasanisi A, Longo F, Gianesin B, Forni GL. Webthal p: revisiting iron overload status and change thresholds as predictors of mortality in transfusion-dependent beta-thalassemia: a 10-year cohort study. Ann Hematol. 2024. https://doi.org/10.1007/s00277-024-05715-x
5. Saravi M, Tamadoni A, Jalalian R, Mahmoodi–Nesheli H, Hojati M, Ramezani S. Evaluation of tissue doppler echocardiography and T2* magnetic resonance imaging in iron load of patients with Thalassemia major. Caspian J Intern Med. 2013;4(3):692.
6. Kirk P, Roughton M, Porter JB, Walker JM, Tanner MA, Patel J, Wu D, Taylor J, Westwood MA, Anderson LJ. Cardiac T2* magnetic resonance for prediction of cardiac complications in Thalassemia major. Circulation. 2009;120(20):1961–8.
7. Modell B, Khan M, Darlison M, Westwood MA, Ingram D, Pennell DJ. Improved survival of Thalassaemia major in the UK and relation to T2* cardiovascular magnetic resonance. J Cardiovasc Magn Reson. 2008;10(1):42. https://doi.org/10.1186/1532-429X-10-42
8. Farmakis D, Porter J, Taher A, Domenica Cappellini M, Angastiniotis M, Eleftheriou A. 2021 Thalassaemia International Federation guidelines for the management of transfusion-dependent thalassemia. Hemasphere. 2022;6(8):e732. https://doi.org/10.1097/HS9.0000000000000732
9. Fernandes JL, Sampaio EF, Verissimo M, Pereira FB, da Silva JA, de Figueiredo GS, Kalaf JM, Coelho OR. Heart and liver T2 assessment for iron overload using different software programs. Eur Radiol. 2011;21(12):2503–10. https://doi.org/10.1007/s00330-011-2208-1
10. Git KA, Fioravante LA, Fernandes JL. An online open-source tool for automated quantification of liver and myocardial iron concentrations by T2* magnetic resonance imaging. Br J Radiol. 2015;88(1053):20150269. https://doi.org/10.1259/bjr.20150269
11. Sagar CS, Kumar R, Sharma DC, Kishor P. DNA damage: beta zero versus beta plus thalassemia. Ann Hum Biol. 2015;42(6):585–8. https://doi.org/10.3109/03014460.2014.990921
12. Lambrou AT, Samartzi GI, Vlachou A, Papassotiriou E, Geronikolou I, Kanaka-Gantenbein SA, Chrousos C, Kattamis GP. Genotypic and clinical analysis of a Thalassemia major cohort: an observational study. Adv Exp Med Biol. 2021;1339:65–76. https://doi.org/10.1007/978-3-030-78787-5_10
13. Pistoia L, Meloni A, Ricchi P, Filosa A, Lisi R, Maggio A, Rosso R, Messina G, Iacono ND, Cuccia L, et al. Genotypic groups as risk factors for cardiac magnetic resonance abnormalities and complications in Thalassemia major: a large, multicentre study. Blood Transfus. 2021;19(2):168–76. https://doi.org/10.2450/2020.0023-20
14. Pistoia L, Meloni A, Salvadori S, Spasiano A, Lisi R, Rosso R, Maggio A, D'Ascola DG, Cuccia L, Mangione M, et al. Cardiac involvement by CMR in different genotypic groups of Thalassemia major patients. Blood Cells Mol Dis. 2019;77:1–7. https://doi.org/10.1016/j.bcmd.2019.01.008
15. Meloni A, Restaino G, Borsellino Z, Caruso V, Spasiano A, Zuccarelli A, Valeri G, Toia P, Salvatori C, Positano V, et al. Different patterns of myocardial iron distribution by whole-heart T2* magnetic resonance as risk markers for heart complications in Thalassemia major. Int J Cardiol. 2014;177(3):1012–9. https://doi.org/10.1016/j.ijcard.2014.09.139
16. Anderson LJ, Holden S, Davis B, Prescott E, Charrier CC, Bunce NH, Firmin DN, Wonke B, Porter J, Walker JM, et al. Cardiovascular T2-star (T2*) magnetic resonance for the early diagnosis of myocardial iron overload. Eur Heart J. 2001;22(23):2171–9. https://doi.org/10.1053/euhj.2001.2822
17. Kirk P, Roughton M, Porter JB, Walker JM, Tanner MA, Patel J, Wu D, Taylor J, Westwood MA, Anderson LJ, et al. Cardiac T2* magnetic resonance for prediction of cardiac complications in Thalassemia major. Circulation. 2009;120(20):1961–8. https://doi.org/10.1161/CIRCULATIONAHA.109.874487
18. Zhou Y, Cao Y, Fang Z, Huang K, Yang M, Pang G, Zhao J, Liu Y, Luo J. Research on the clinical factors of cardiac iron deposition in children with beta-thalassemia major. Eur J Pediatr. 2024;183(2):875–82. https://doi.org/10.1007/s00431-023-05300-w
19. El Sherif AM, Ibrahim AS, Elsayed MA, Abdelhakim AS, Ismail AM. The impact of magnetic resonance imaging in the assessment of iron overload in heart and liver in transfusion-dependent thalassemic children: Minia experience. Egypt J Radiol Nuclear Med. 2021;52(1). https://doi.org/10.1186/s43055-021-00645-4
20. Xu F, Li D, Tang C, Liang B, Guan K, Liu R, Peng P. Magnetic resonance imaging assessment of the changes of cardiac and hepatic iron load in Thalassemia patients before and after hematopoietic stem cell transplantation. Sci Rep. 2023;13(1):19652. https://doi.org/10.1038/s41598-023-46524-y
21. Ouederni M, Ben Khaled M, Mellouli F, Ben Fraj E, Dhouib N, Yakoub IB, Abbes S, Mnif N, Bejaoui M. Myocardial and liver iron overload, assessed using T2* magnetic resonance imaging with an Excel spreadsheet for post processing in Tunisian Thalassemia major patients. Ann Hematol. 2017;96(1):133–9. https://doi.org/10.1007/s00277-016-2841-5
22. Ansah D, Husain N, Ruh A, Berhane H, Smith A, Thompson A, De Freitas A, Rigsby CK, Robinson JD. Cardiac magnetic resonance strain in beta Thalassemia major correlates with cardiac iron overload. Child (Basel). 2023;10(2). https://doi.org/10.3390/children10020271
23. Di Maggio R, Maggio A. The new era of chelation treatments: effectiveness and safety of 10 different regimens for controlling iron overloading in Thalassaemia major. Br J Haematol. 2017;178(5):676–88. https://doi.org/10.1111/bjh.14712
24. Bardon-Cancho EJ, Marco-Sanchez JM, Beneitez-Pastor D, Payan-Pernia S, Llobet AR, Berrueco R, Garcia-Morin M, Belendez C, Senent L, Acosta MJO, et al. Spanish registry of hemoglobinopathies and rare anemias (REHem-AR): demographics, complications, and management of patients with beta-thalassemia. Ann Hematol. 2024. https://doi.org/10.1007/s00277-024-05694-z
25. Reddy PS, Locke M, Badawy SM. A systematic review of adherence to iron chelation therapy among children and adolescents with thalassemia. Ann Med. 2022;54(1):326–42. https://doi.org/10.1080/07853890.2022.2028894
26. Pepe A, Meloni A, Capra M, Cianciulli P, Prossomariti L, Malaventura C, Putti MC, Lippi A, Romeo MA, Bisconte MG, et al. Deferasirox, deferiprone and desferrioxamine treatment in Thalassemia major patients: cardiac iron and function comparison determined by quantitative magnetic resonance imaging. Haematologica. 2011;96(1):41–7. https://doi.org/10.3324/haematol.2009.019042
27. Ricchi P, Meloni A, Pistoia L, Gamberini MR, Cuccia L, Allo M, Putti MC, Spasiano A, Rosso R, Cecinati V, et al. Longitudinal prospective comparison of pancreatic iron by magnetic resonance in Thalassemia patients transfusion-dependent since early childhood treated with combination deferiprone-desferrioxamine vs deferiprone or deferasirox monotherapy. Blood Transfus. 2024;22(1):75–85. https://doi.org/10.2450/BloodTransfus.485

28. Carpenter JP, He T, Kirk P, Roughton M, Anderson LJ, de Noronha SV, Sheppard MN, Porter JB, Walker JM, Wood JC, et al. On T2* magnetic resonance and cardiac iron. Circulation. 2011;123(14):1519–28. https://doi.org/10.1161/CIRCULATIONAHA.110.007641